Mechanics of Advanced Composite Structures 4 (2017) 117-125

Semnan University

Mechanics of Advanced Composite Structures

journal homepage: http://MACS.journals.semnan.ac.ir

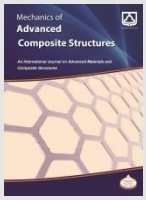

Numerical Simulation of a Hybrid Nanocomposite Containing CaCO3 and Short Glass Fibers Subjected to Tensile Loading

M.D. Shokrian*, K. Shelesh-Nezhad, B.H. Soudmand

Department of mechanical engineering, University of Tabriz, Tabriz 51666-1476, Iran

PAPER INFO

Paper history:
Received 2016-12-01
Revised 2017-03-23
Accepted 2017-04-03

Keywords:
Hybrid thermoplastic nanocomposites
Effective matrix
Finite element method
Tensile properties

ABSTRACT

The tensile properties of multiscale, hybrid, thermoplastic-based nanocomposites reinforced with nano-$CaCO_3$ particles and micro–short glass fibers (SGF) were predicted by a two-step, three-dimensionalmodel using ANSYS finite element (FE) software. Cylindrical and cuboid representative volume elements were generated to obtain the effective behavior of the multiscale hybrid composites. In the first step, the mechanical performance of co-polypropylene/$CaCO_3$ nanocomposite was analyzed. The thickness of the interphase layer around the nanoparticles was estimated by using differential scanning calorimetry data. In the second step, the nanocomposite (co-polypropylene/$CaCO_3$) was considered as an effective matrix, and then the effect of micro-SGF inclusion on the corresponding effective matrix was evaluated. The FE and experimental stress-strain curves of multiscale, hybrid composites were compared at different weight fractions of the nanoparticle. The proposed two-step method can easily predict the tensile properties of multiscale, hybrid, thermoplastic-based nanocomposites.

1. Introduction

The simultaneous use of different scaled reinforcements in polymer composites introduced novel polymer composite materials in the field of material science and technology. Hybrid composite systems consisting of different kinds of reinforcing materials have become attractive due to the synergy of their ingredients. This synergy is often called the "hybrid effect" [1, 2]. Consequently, considerable attention has been given to the performance of these composites. Liu et al. [3] observed a synergistic effect in simultaneous improvements in the wear and mechanical properties of high-density polyethylene (HDPE) by applying graphitic nanoplatelets and graphite nanofibers into a neat polymer. A study by Karsli et al. [4] revealed that the concurrent addition of glass fibers and carbon nanotubes into a polypropylene (PP) matrix increases the reinforcing ability of nanotubes in polymer composites. Pedrazzoli and Pegoretti [5] found that the interfacial strength of glass fiber/PP composites was remarkably increased by the hybridization of silica nanoparticles. Thostenson et al. [6] indicated that the incorporation of carbon nanotubes into carbon fiber composites stiffened the polymer matrix near the fiber/matrix interface, thereby improving interfacial load transfer. Hartikainen et al. [7] demonstrated that adding $CaCO_3$ nanoparticles into long glass fiber and PP composites increased stiffness, although it also decreased strength. The hybridization of short glass fibers (SGF) and inorganic particles in Pande and Sharma's research showed advantages in tensile strength and stiffness over using fillers alone in a PP matrix [8]. Hence, it can be concluded that positive and negative effects on the tensile strength of hybrid composites depend on reinforcements and matrix characteristics [9].

Due to the difficulties involved in experimental characterizations, analytical and numerical simulations are becoming more attractive compared to experimental alternatives. The simplest method for predicting the strength and modulus of hybrid composites is the Rule of Hybrid Mixtures (RoHM) equation. The RoHM is widely used by researchers. Venkateshwaran et al. [10] tried to evaluate the tensile properties of randomly oriented, natural fiber–reinforced hybrid composites by applying the RoHM. They observed that by using the RoHM equation, the calculated tensile properties of hybrid composites

* Corresponding author, Tel.: +98-9379918820

E-mail address: md.shokrian@tabrizu.ac.ir

were slightly higher than experimental values. A similar method was used by Fu et al. [11] to predict the elastic modulus of hybrid ABS/particle/SGF polymer composite. By using the RoHM equation, the effective elastic properties were calculated as a function of only elastic properties and reinforcement volume fractions. Therefore, the influence of many effective phenomena, such as the interphase layer, was ignored, and the prediction error was increased. Moreover, tough, thermoplastic-based composites show completely nonlinear elastic behavior. Therefore, considering the stress-strain curves of composites instead of calculating the slope of stress-strain curves as the modulus is preferred for materials.

The laminating analogy approach (LAA), a theoretical platform, was also used to evaluate the mechanical properties of hybrid composites. Lee et al. [1] applied the LAA to estimate the overall elastic modulus of multiphase hybrid composites filled with talc particles and glass fibers. Lee et al. [12] further proposed a statistical model by adopting the log-normal and generalized extreme value (GEV) functions to predict the effective elastic moduli of multiphase hybrid composites. Their theoretical results agreed with the experimental data. Recently, an analytical-stochastic, multiscale, computational model was suggested by Guan et al. [13] for predicting the tensile properties of fiber-reinforced concrete. Nonetheless, in the previous research, the effect of the interphase layer on the tensile properties of hybrid composites was neglected. Moreover, rare works have been reported on finite element (FE) modeling of hybrid thermoplastic nanocomposites.

It is well known that the interphase layer of a composite controls its mechanical properties, especially in the case of polymers reinforced by nanoparticles. Many considerable studies have been carried out in the literature to show the importance of the interphase layer in nanocomposites [14, 15]. Zamani-Zakaria and Shelesh-Nezhad [16] demonstrated that interphase properties could influence the tensile modulus of POM/$CaCO_3$ nanocomposites. The properties of the interphase layer itself depend on many factors, such as the properties of the matrix and reinforcement, the rate of solidification, filler content, and the sizing characteristics of filler [17]. Some researchers have used molecular dynamics simulation [18-20], dynamic mechanical analysis [21], inverse FEM [22], differential scanning calorimetry data [23], and the developed form of Leidner-Woodhams and Pukanszky models [24] to predict the interphase thickness of nanoparticles.

The objective of this research was to simulate the tensile behavior of multiscale hybrid nanocomposites using a two-step, FE model. Similar to the preparation process of a hybrid composite, in the first step, the tensile properties of a nanocomposite system are modeled. In the second step, the nanocomposite-containing polymer matrix and nanoparticles that were modeled in the first step are considered as an effective matrix, and then the fiber and its interaction with the effective matrix are simulated. To validate the ability of the proposed method to estimate the tensile properties of hybrid thermoplastic nanocomposites, FE predictions were compared with those of micromechanical methods and experiments.

2. Experimental

High-impact polypropylene (Jampilen EP440L) was employed as the polymer matrix. Nano-$CaCO_3$ particles (NPCC-201) 10 nm in diameter were used as nano-reinforcement. SGF (144A- Taiwan Glass) with a nominal diameter of 13 μm and a length of 3.2–4.8 mm were incorporated into the matrix. PP-g-MAH was used as a sizing agent for both $CaCO_3$ nanoparticles and glass fibers. The hybrid nanocomposites contain 10 wt% of SGF and 2, 5, and 8 wt% of $CaCO_3$ nanoparticles. At the first stage of melt compounding, co-PP/$CaCO_3$ nanocomposites were produced. At the second stage of extrusion, fibers were added to the aforementioned compound. Tensile test specimens were prepared according to ISO 527 by an injection molding machine (H 485 / 140 TP). Tensile tests were performed with a speed of 50 mm/min and a gauge length of 50 mm.

3. Finite Element Modeling

In order to examine the influence of both particles and fibers on the composite's tensile properties, an effective hybrid method [1] was adopted using a two-step FE simulation. Figure 1 represents a schematic illustration of the simulation process. In order to simulate the multiscale hybrid material, first, a system containing nano-$CaCO_3$ and PP was modeled. At the second stage, the predicted tensile properties of the aforementioned nanocomposite were considered as effective matrix properties, and the corresponding effective matrix interaction with fiber was simulated, as shown in Figure 1.

One of the simple numerical models developed in the literature to compute the tensile properties of composites is based on the assumption of periodically distributed reinforcements dispersed in a continuous matrix [25]. In order to reflect this assumption, a cubic or cylindrical representative volume element (RVE) may be used [14, 26-28]. Due to the spherical geometry of nano-$CaCO_3$ particles, a cylindrical, single-particle RVE (*RVE1*) was used in the current research to model a nano-$CaCO_3$ particle/polymer system, as shown in Figure 2.

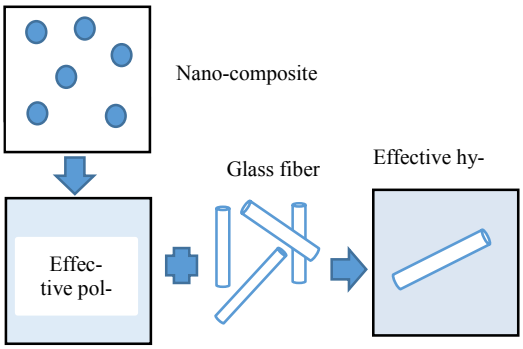

Figure 1. Schematic illustration of the hybrid system modeling.

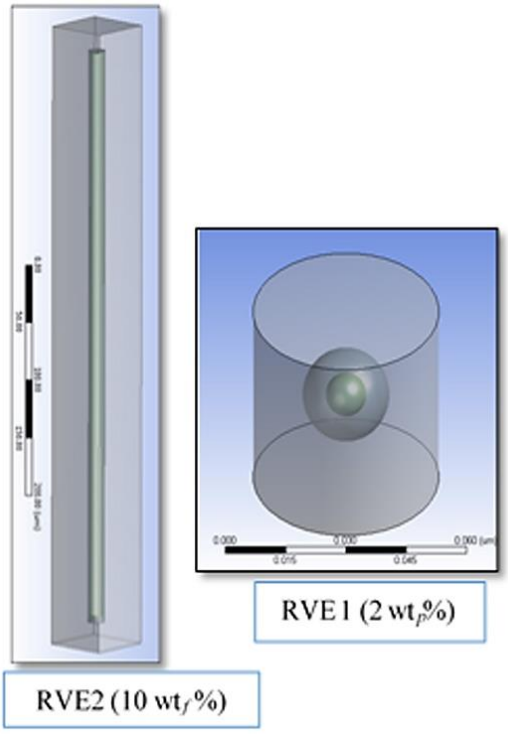

Figure 2. Cylindrical and cuboid RVEs.

A cuboid RVE (*RVE2*) containing a cylindrical SGF was also adopted for fiber/effective matrix–composite system modeling, also shown in Figure 2. Determining the RVE dimensions required the establishment of the particle volume fraction (V_p) and fiber volume fraction (V_f) using weight fractions (wt) of both reinforcements by employing equation (1) and (2) [14, 29]:

$$V_p = \frac{wt_p/\rho_p}{wt_p/\rho_p + (1-wt_p)/\rho_m}, \quad (1)$$

$$V_f = \frac{wt_f/\rho_f}{wt_p/\rho_p + wt_f/\rho_f + (1-wt_p-wt_f)/\rho_m}, \quad (2)$$

where ρ is density. Subscript m, p, and f refer to matrix, particle, and fiber properties, respectively. By considering the fact that the ratio of particle volume to RVE1 volume is equal to V_p, the radius (r_{RVE1}) and length (l_{RVE1}) of cylindrical RVE1 can be calculated using equation (3).

$$r_{RVE1} = \sqrt[3]{2r_p^3/3V_p} \quad and \quad l_{RVE1} = 2r_{RVE1}. \quad (3)$$

Similar to that of RVE1, the ratio of fiber volume to RVE2 volume is equal to V_f, hence, the dimensions of the effective cuboid RVE2 can be obtained from equation (4) [30]:

$$V_f = \frac{\pi r_f^2 l_f}{a_{RVE2}^2 b_{RVE2}} \quad \begin{cases} a_{RVE2} = 2(r_f + s) \\ b_{RVE2} = l_f + 2s \end{cases}, \quad (4)$$

where l, a, and b are length, side, and height, respectively. The variable s is the distance between fiber and RVE2 surfaces. By substituting the a_{RVE2} and b_{RVE2} terms in equation (4), a third-order polynomial equation is obtained (equation [5]). By solving equation (6), three roots are yielded for s that only positive one is acceptable.

$$s^3 + As^2 + Bs + C = 0,$$
$$A = 0.5l_f + 2r_f,$$
$$B = r_f l_f + r_f^2,$$
$$C = 0.5r_f^2 l_f (1 - \pi/(4V_f)). \quad (5)$$

To model the tensile properties of co-PP, the behavior of the polymer matrix material was assumed to be isotropic and elastic-plastic [26]. The engineering stress-strain curve of tensile test for neat co-PP was extracted from experiments performed according to ISO 527 and then was converted to the true stress-strain data using Ling's weighted-average method [31]. The material properties of the particle, fiber, and interphases were assumed to be linear, elastic, and isotropic [32, 33]. Because of the high shear stress involved in the melt processing as well as the brittle nature of glass fibers, glass fibers are broken over the melt compounding. This may lead to the shortening of the glass fibers to about 0.4 mm [11]. Table 1 shows the properties of the polymer, particle, and fiber used in this paper.

Table 1. Material properties.

Property	E (GPa)	ν	Density (g/cm³)	Dimension
Co-PP	0.435	0.45	0.9	-
Nano-$CaCO_3$	179[a]	0.3	2.7	$r_p = 5$ nm
Glass fiber	75[b]	0.25	2.58	$r_f = 6.5$ μm , Aspect ratio=31

[a] reference [28]. [b] reference [34].

Due to the thinness of the interphase layer in nanocomposite, the characterization of the interphase is a difficult task that cannot be carried out directly from experiments [35]. Therefore, making assumptions about the interphase properties may be required [36]. As a result, due to a lack of interphase properties, most researchers suggest a constant value for the interphase thickness of nanocomposites (for different weight fractions of particles) in FE simulations [37].

To establish the interphase thickness in this research, it was assumed that the improvement in crystallinity of the composite, induced by the nucleating effect of the nanoparticle, led to the formation of an interphase layer in the vicinity of the nanoparticle. Based on the aforementioned assumption, the volume fraction of the interphase layer was considered to be equal to the improvement in crystallinity (ΔX) because of the addition of nanoparticles to the pure polymer. Therefore, the thickness of nano-interphase, t_{RVE1}, was derived by using equation (6).

$$\Delta X = V_i = \frac{(r_p + t_{RVE1})^3 - r_p^3}{1.5\, r_{RVE1}^3 - r_p^3},$$
$$\Delta X = Xc_{composites} - Xc_{polymer}, \quad (6)$$

where $Xc_{composites}$ and $Xc_{polymer}$ are the crystallinity degrees of nanocomposites and neat co-PP, respectively. The values of $Xc_{polymer}$ and $Xc_{composites}$ for different weight fractions of nano-$CaCO_3$ were obtained by differential scanning calorimetry (DSC) with the thermo-analytical tester model TOLEDO (METTLER German). The crystallinity improvements and the interphase thicknesses of RVE1, calculated using equation (6), are presented in Table 2 (where $Xc_{polymer} = 31\%$).

In order to calculate the interphase thickness of microfiber, the volume fraction of the interphase layer in RVE2 was assumed to be 2% [38].

Table 2. Crystallinity improvements and interphase thicknesses of nanocomposites.

Nanoparticles (wt%)	ΔX (%)	t_{RVE1} (nm)
2	6.09	5.75
5	1.87	1.3
8	4.26	1.75

The elastic modulus (E) and the Poisson's ratio (ν) of the interphase layer for both RVE1 and RVE2 were assumed to vary continuously along the thickness where their boundary values were considered to be equal to those of the matrix and reinforcements (equation [7]) [16, 36].

$$H_i(r)/H_m = 1 + \left(\frac{H_{p\ or\ f}}{H_m} - 1\right)\frac{1 - (r/r_i)exp(1 - (r/r_i))}{1 - (r_{p\ or\ f}/r_i)exp(1 - (r_{p\ or\ f}/r_i))}, \quad (7)$$

where H is either E or ν. Subscript i refers to the interphase properties. The average value of H_i, used to homogenize the properties of the interphase layer, can be obtained by integrating equation (7), ranging from the radius of reinforcements to the radius of the interphase (equation [8]).

$$H_i = \frac{1}{r_i - r_f}\int_{r_f}^{r_i} H_i(r)\, dr. \quad (8)$$

Perfect bonds between polymer and inclusions were assumed as reported by Zuberi and Esat [39]. Therefore, the predicted tensile strength was only related to the matrix yielding. Since the unit cells were symmetrical, an eighth of the RVEs were analyzed. The model was then meshed using SOLID187 for matrix and interphase and SOLID186 for fiber and particle. TARGE170 and CONTA174 were simultaneously applied to define the connections in the interfaces. Typical FE mesh was used, which was strongly refined near the interface region and particle. For both RVE1 and RVE2, displacement boundary conditions were applied as shown in Figure 3.

4. Results and Discussion

Experimental tensile tests were repeated five times, and median stress-strain curves and the corresponding moduli were depicted and compared with FE simulations. FE models with different weight fractions of reinforcements were created and analyzed using the commercial ANSYS FE analysis software. In FE simulation, the amount of deformation divided by the initial length of RVE gave strain.

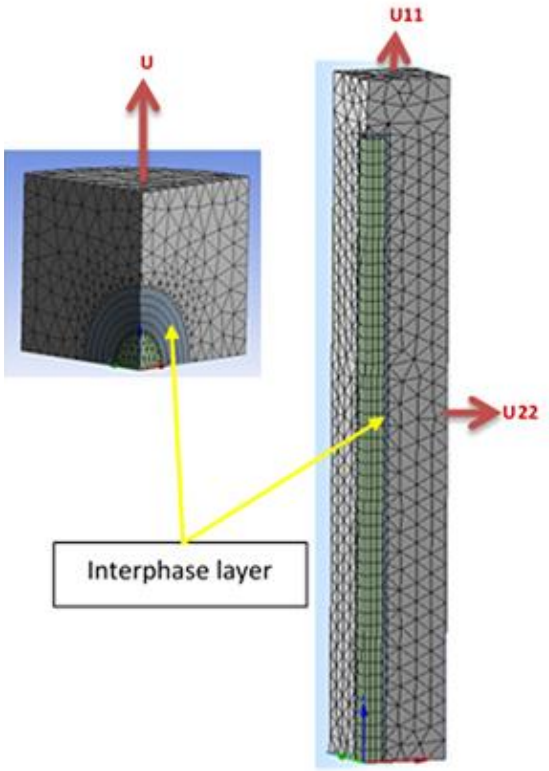

Figure 3. Illustrations of the 1/8 RVEs, refined meshes and displacement boundary conditions.

Figure 4 presents the engineering stress-strain curves of nanocomposites that resulted from the experimental tests and FE simulations. For all nanocomposites, it can be seen that the FE data within the elastic region, as compared to the plastic region, closely matched the experimental results. This is due to the complexity of plastic deformation in comparison with elastic deformation in polymers. According to Figure 4(a), at large strain values (strains higher than about 0.2) the FE simulation of the elastic-plastic model was unable to accurately predict the tensile behavior of large-deformable neat co-PP, where localized necking in the cross section of RVE appeared and developed rapidly at large plastic strains. However, the incorporation of nano-$CaCO_3$ into co-PP and the presence of the interphase layer in the RVE delayed necking, and this delay allowed the composite to bear higher stress prior to failure. In general, the comparison between experimental and FE engineering stress-strain curves revealed that the nanocomposites containing 5 and 8 wt% of $CaCO_3$ showed less deviation than the composite filled with 2 wt% of $CaCO_3$. Most probably, in the nanocomposite containing 2 wt% of $CaCO_3$, interphase percolation occurred, which may have led to the improved tensile properties of the composite. Interphase percolation is defined as overlapping particle interphases, and it forms when the interphase volume fraction or thickness is relatively high [40, 41]. According to Table 2, the thickest interphase belonged to the nanocomposite with 2 wt% of $CaCO_3$. This may increase the tendency of particles' interphase percolation. In this work, the FE simulation of nanocomposites was done using single-particle RVE and, hence, the interphase percolation was ignored.

Figure 5 compares the experimental and two-step FEM engineering stress-strain curves along and across the fiber directions of hybrid nanocomposites. The results of two-step modeling show that the tensile strength along the transverse direction was higher than along the longitudinal direction. Moreover, the RVE of hybrid nanocomposites along the transverse direction exhibited tough behavior. The comparison of different experimental and FE simulation stress-strain curves revealed that strength values that resulted from experiments were more than those obtained by FEM. This deviation for co-PP/10 wt% and SGF/5 wt% $CaCO_3$ was relatively higher than others, as shown in Figure 5(c). The tough behavior of the polymer matrix, i.e., co-PP, may be a source of prediction error in FE11 modeling. Another source of prediction error can be attributed to neglecting the direct interaction of nano-$CaCO_3$ particles with SGFs. Although the two-step FEM presents the benefits of FEM in simulating multiscale hybrid nanocomposites, it disregards the direct interactions between particles and fibers. By comparing the results of FE simulations with those of experiments for both naonocomposites and hybrid nanocomposites (see Figures 4 and 5), it can be concluded that the main part of the discrepancy that occurred relates to the simulation of the fiber/matrix RVE.

Figure 6 compares the elastic moduli (the slopes of the stress-strain curves in the region of 0 to 0.003 strain) of different hybrid nanocomposites (containing 10 wt% of fibers) as a result of FEM and modified RoHM theory when the particle reinforcing factor = 0.1 and the fiber reinforcing factor = 0.1 in the transverse direction and 0.5 in the longitudinal direction [42]. The reinforcing factor or efficiency factor of reinforcement, depending on the reinforcement's orientation and length or geometry factors, has a value between 0 and 1 [11, 42]. From Figure 6, the predicted modulus values using two-step FEM is relatively close to the RoHM values. It is worth noting that the transverse modulus (E22) of the hybrid composite is obviously lower than the longitudinal modulus (E11) for both approaches. So, hybrid nanocomposites display stiffer behavior along the fiber direction as compared to that of the transverse direction [30].

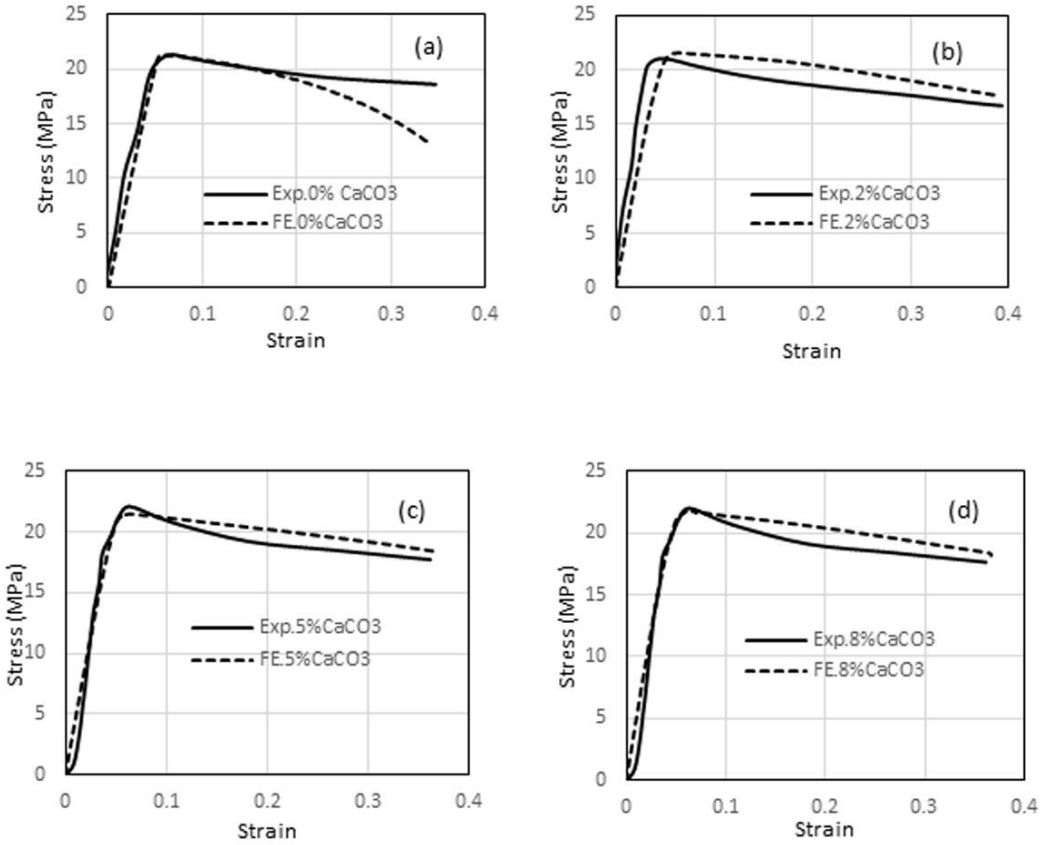

Figure 4. Engineering stress-strain curves of nanocomposite at: (a) 0, (b) 2, (c) 5, (d) 8 wt% of the particle (Exp. and FE refer to experimental and FE results, respectively).

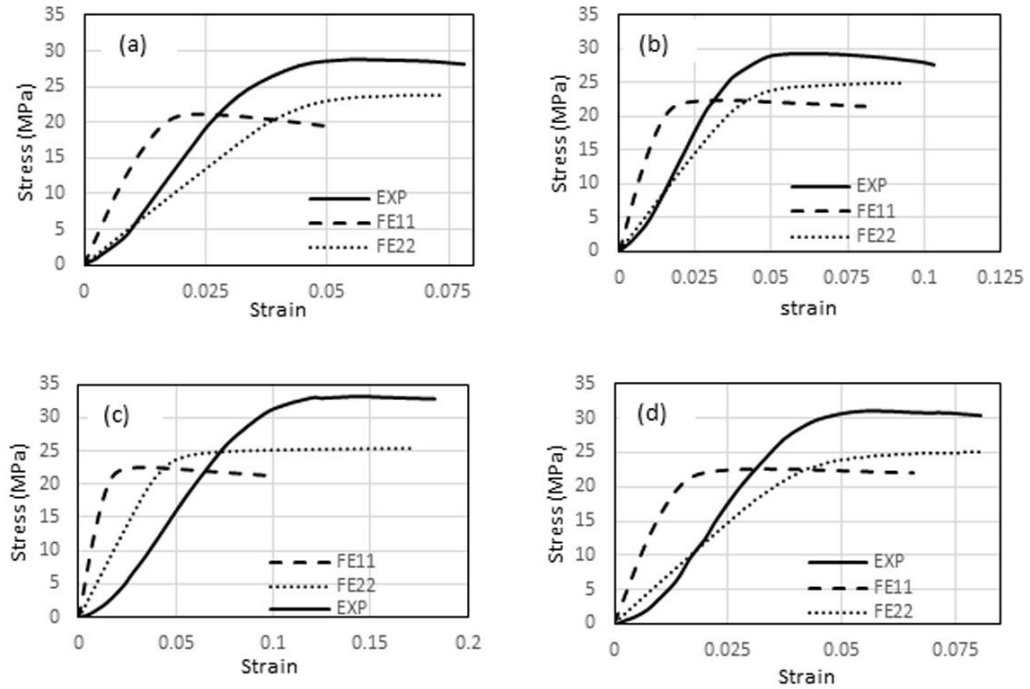

Figure 5. Engineering stress-strain curves predicted by FEM against experimental testes for hybrid nanocomposites reinforced by 10 wt% of SGF containing: (a) 0, (b) 2, (c) 5, (d) 8 wt% of particle. FE11: longitudinal direction, FE22: transverse direction.

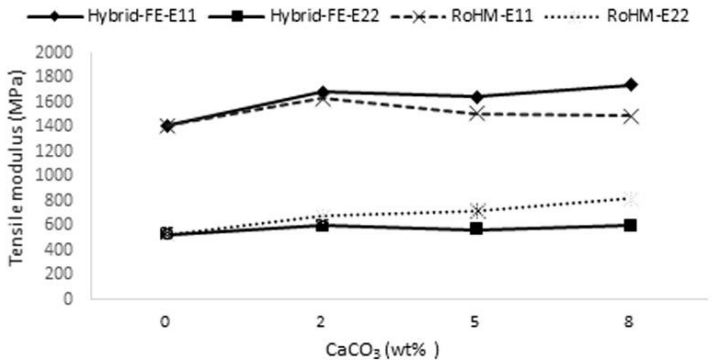

Figure 6. Comparison of hybrid FE simulation moduli with RoHM, 10 wt% of fibers.

5. Conclusion

In the present study, multiscale reinforcements filled co-PP consisting of CaCO3 nanoparticles, and micron SGF was simulated via a two–step FE model using a 3D RVE. Similar to the preparation process of a hybrid composite, in the first step, the tensile properties of the nanocomposite system were modeled. In the second step, the nanocomposite modeled in the first step was considered as an effective matrix, and then the fiber and its interaction with the effective matrix were simulated. The interphase characteristics were brought into account in FE modeling. Crystallinity data obtained by DSC thermo-analytical tests was employed to acquire the interphase thickness of nanocomposites. The FE simulations demonstrated that glass fibers in the longitudinal direction make hybrid composites stiffer. Higher tensile strength as well as toughness was achieved in the transverse direction of glass fibers. The FE and the experimental stress-strain curves of hybrid composites were compared at different weight fractions of nanoparticle. The stress- strain data obtained by FEM showed less deviation from experiments in the elastic region as compared to that of plastic region. The FE simulation of the nanocomposite in comparison to the hybrid composite showed better agreement with experiments. However, the proposed two-step approach is comparatively simple and more accurate than traditional micromechanical methods in evaluating the tensile behavior of especially tough, thermoplastic-based hybrid nanocomposites. The two-step FE mod of hybrid composites has the potential to be further improved by deepening the FE modeling of fiber/matrix.

References

[1] Lee DJ, Oh H, Song YS, Youn JR. Analysis of effective elastic modulus for multiphased hybrid composites. *Compos Sci Technol* 2012; 72(2):278-283.

[2] Wan T, Liao S, Wang K, Yan P, Clifford M. Multiscale hybrid polyamide 6 composites reinforced with nano-scale clay and micro-scale short glass fibre. *Compos Part A: Appl Sci Manuf* 2013; 50:31-38.

[3] Liu T, Wang Y, Eyler A, Zhong W-H. Synergistic effects of hybrid graphitic nanofillers on simultaneously enhanced wear and mechanical properties of polymer nanocomposites. *Eur Polym J* 2014; 55:210-221.

[4] Karsli NG, Yesil S, Aytac A. Effect of hybrid carbon nanotube/short glass fiber reinforcement on the properties of polypropylene composites. *Compos Part B* 2014; 63:154-160.

[5] Pedrazzoli D,Pegoretti A. Silica nanoparticles as coupling agents for polypropylene/glass composites. *Compos Sci Technol* 2013; 76:77–83.

[6] Thostenson ET, Li WZ, Wang DZ, Ren ZF, Chou TW. Carbon nanotube/carbon fiber hybrid multiscale composites *J Appl Phys* 2002; 91(9).

[7] Hartikainen J, et al. Polypropylene hybrid composites reinforced with long glass fibres and particulate filler. *Compos Sci Technol* 2005; 65(2):257-267.

[8] Pande S,Sharma D. Strength and stiffness of short glass fibre/glass particulate hybrid composites. *Fibre Sci Technol* 1984; 20:235–43.

[9] Szeluga U, Kumanek B, Trzebicka B. Synergy in hybrid polymer/nanocarbon composites. A review. *Compos Part A* 2015; 73:204-231.

[10] Venkateshwaran N, Elayaperumal A, Sathiya GK. Prediction of tensile properties of hybrid-natural fiber composites. *Compos Part B* 2012; 43:793-796.

[11] Fu S-Y, Xu G, Mai Y-W. on the elastic modulus of hybrid particle/short-fiber/polymer composites. *Compos Part B* 2002; 33.

[12] Lee DJ, Hwang SH, Song YS, Youn JR. Statistical modeling of effective elastic modulus for multiphased hybrid composites. *Polym Testing* 2015; 41:99-105.

[13] Guan X, et al. A stochastic multiscale model for predicting mechanical properties of fiber reinforced concrete. *Int J Solids Struct* 2015; 56–57:280-289.

[14] Pontefisso A, Zappalorto M, Quaresimin M. Influence of interphase and filler distribution on the elastic properties of nanoparticle filled polymers. *Mech Res Commun* 2013; 52:92-94.

[15] Boutaleb S, et al. Micromechanical modelling of the yield stress of polymer-particulate nanocomposites with an inhomogeneous interphase. *Procedia Eng* 2009; 1(1):217-220.

[16] Zamani-Zakaria A,Shelesh-Nezhad K. The Effects of Interphase and Interface Characteristics on the Tensile Behaviour of POM/CaCO3 Nanocomposites. *Nanomaterials and Nanotechnology* 2014; 14(17):1–10.

[17] Sattaria M, Naimi-Jamal MR, Khavandi A. Interphase evaluation and nano-mechanical responses of UHMWPE / SCF / nano-SiO2hybrid composites. *Polym Testing* 2014; 38:26-34.

[18] Hadden CM, et al. Molecular modeling of EPON-862/graphite composites: Interfacial characteristics for multiple crosslink densities. *Compos Sci Technol* 2013; 76(0):92-99.

[19] Choi J, Shin H, Yang S, Cho M. The influence of nanoparticle size on the mechanical properties of polymer nanocomposites and the associated interphase region: A multiscale approach. *Compos Struct* 2015; 119(0):365-376.

[20] Tsai J-L,Tzeng S-H. Characterizing mechanical properties of particulate nanocomposites using micromechanical approach. *J Compos Mater* 2008; 42(22):2345-2361.

[21] Arrighi V, Mcewen IJ, H.Qian, Prieto MBS. The glass transition and interfacial layer in styrene-butadiene rubber containing silica nanofiller. *Polym* 2003; 44(20):6259-6266.

[22] Jang J-S, Bouveret B, Suhr J, Gibson RF. Combined numerical/experimental investigation of particle diameter and interphase effects on coefficient of thermal expansion and young's modulus of SiO2/epoxy nanocomposites. *Polym Compos* 2012; 33(8):1415–1423.

[23] Zamani-Zakaria A, F MS, Shelesh-Nezhad K. A combined numerical and experimental study for characterizing interfacial properties of polyoxymethylene–calcium carbonate nanocomposites in tensile state. *J Compos Mater* 2015; 0:1-10.

[24] Zare Y. Modeling the strength and thickness of the interphase in polymer nanocomposite reinforced with spherical nanoparticles by a coupling methodology. *J Colloid Interface Sci* 2016; 465:342-346.

[25] Hutar P, Náhlík L, Majer Z, Knésl Z. **5-The Effect of an Interphase on Micro-Crack Behaviour in Polymer Composites**, in Computational Modelling and Advanced Simulations, Springer Science+Business Media B.V;2011.

[26] Zeng X, Fan H, Zhang J. Prediction of the effects of particle and matrix morphologies on Al2O3 particle/polymer composites by finite element method. *Comput Mater Sci* 2007; 40(3):395-399.

[27] Chang S, Yang S, Shin H, Cho M. Multiscale homogenization model for thermoelastic behavior of epoxy-based composites with polydisperse SiC nanoparticles. *Compos Struct* 2015; 128:342-353.

[28] Kemal I, Whittle A, Burford R, Vodenitcharova T, Hoffman M. Toughening of unmodified polyvinylchloride through the addition of nanoparticulate calcium carbonate. *Polym* 2009; 50(16):4066-4079.

[29] Wang K, et al. Micromechanical modeling of the elastic behavior of polypropylene based organoclay nanocomposites under a wide range of temperatures and strain rates/frequencies. *Mech Mater* 2013; 64:56-68.

[30] Shokrian MD, Shelesh-Nezhad K, Soudmand BH. 3D FE analysis of tensile behavior for co-PP/SGF composite by considering interfacial debonding using CZM. *J Reinforced Plastics Compos* 2015.

[31] Ling Y. Uniaxial True Stress-Strain after Necking. *AMP J Technol* 1996; 5:34-48.

[32] Wongsto A, Li S. Micromechanical FE analysis of UD fibre-reinforced composites with fibres distributed at random over the transverse cross-section. *Compos Part A: Appl Sci Manuf* 2005; 36(9):1246-1266.

[33] Pisano C, Priolo P, Figiel Ł. Prediction of strength in intercalated epoxy–clay nanocomposites via finite element modelling. *Comput Mater Sci* 2012; 55:10-16.

[34] Lu Z, Yuan Z, Liu Q. 3D numerical simulation for the elastic properties of random fiber composites with a wide range of fiber aspect ratios. *Comput Mater Sci* 2014; 90:123–129.

[35] Ayatollahia MR, Shadloua S, Shokrieh MM. Multiscale modeling for mechanical properties of carbon nanotube reinforced nanocomposites subjected to different types of loading. *Compos Struct* 2011; 93:2250–2259.

[36] Romanowicz M. Progressive failure analysis of unidirectional fiber-reinforced polymers with inhomogeneous interphase and randomly distributed fibers under transverse tensile loading. *Compos Part A: Appl Sci Manuf* 2010; 41(12):1829-1838.

[37] Peng RD, Zhou HW, Wang HW, Mishnaevsky L. Modeling of nano-reinforced polymer composites: Microstructure effect on Young's modulus. *Comput Mater Sci* 2012; 60:19-31.

[38] Fisher FT,Brinson LC. Viscoelastic interphases in polymer–matrix composites: theoretical models and finite-element analysis. *Compos Sci Technol* 2001; 61.

[39] Zuberia MJS,Esat V. Investigating the mechanical properties of single walled carbon nanotube reinforced epoxy composite through finite element modelling. *Compos Part B* 2015; 71:1–9.

[40] Qiao R,Brinson C. Simulation of interphase percolation and gradients in polymer nanocomposites. *Compos Sci Technol* 2009; 69(3-4):491-499.

[41] Zamani Zakaria A,Shelesh-Nezhad K. Quantifying the particle size and interphase percolation effects on the elastic performance of semi-crystalline nanocomposites. *Comput Mater Sci* 2016; 117:502-510.

[42] Fu S-Y,Lauke B. Characterization of tensile behaviour of hybrid short glass fibre/calcite particle/ABS composites. *Compos Part A: Appl Sci Manuf* 1998; 29(5–6):575-583.